Commutation Control of an MRI-Powered and Imaged Actuator

Ouajdi Felfoul, Alina Eqtami, Aaron Becker, and Pierre E. Dupont

***Abstract*— Actuators that are powered, imaged, and controlled by Magnetic Resonance (MR) scanners offer the potential of inexpensively providing wireless control of MR-guided robots. Similar to traditional electric motors, the MR scanner acts as the stator and generates propulsive torques on an actuator rotor containing one or more ferrous particles.**

I. TASKS

1) Debug the sequence that avoids the two-actuation cycle delay in applying rotor angle.
2) Estimator tasks (most of these are to generate text for paper as well as to justify approach):
   a) (i) Write out an explanation of what type of estimator will work best for our nonlinear system (Extended Kalman filter, particle filter, etc.) (ii) Explain any linearization / operating point that needs to be used. (iii) Write down general equations for selected estimator and then tailor them to our problem. (iv) Account for measurement delay between projections. (iv) Write out entire controller as generic algorithm code (as computer scientists do)
3) Once we are convinced that estimator and controller are correct (by performing tasks above), collect data comparing open- and closed-loop performance of rotor. Important data will include maximum torque produced (stall torque), rotor slip versus no slip, angle between gradient and rotor versus time, effect of actuation duration on stall torque and transient performance, demonstration of position control by step response.
4) Alina could you derive some sort of stability / error bound that we could validate experimentally? If so, what would the validation experiment entail?

II. INTRODUCTION

Robotics offers important contributions to image-guided, minimally invasive surgery. Among imaging techniques, MRI has several advantages. MRI provides high resolution soft-tissue imaging and does not use ionizing radiation.

MRI image-guided procedures, however, pose several challenges for robotics [**?**], [**?**], [**?**], [**?**], [**?**]. First, all ferrous materials create imaging artifacts. Ferrous materials must be isolated from the imaging region of interest. Moreover, the magnetic fields used in an MRI induce forces on any ferrous materials in the robot and turn these materials into strong magnetic dipoles that exert forces on each other. MRI gradients induce current in any conducting materials, which can generate dangerous amounts of heat and also exert forces.

Despite these challenges, there are a number of recent innovations demonstrating tetherless and inexpensive actuation imaged, powered, and controlled using MRI. Martel et al. demonstrated in vivo motion control of a mm-scale particle in the carotid artery of swine [**?**]. Vartholomeos et al. designed a single-DOF MRI-powered actuator for use as a tetherless biopsy robot [**?**]. This was extended to closed-loop control of a single rotor in [**?**]. Since such results require only scanner software and inexpensive actuator components, dissemination of MRI-based robotic technology has the potential to be rapid and inexpensive.

O. Felfoul, A. Eqtami, A. Becker, and P. E. Dupont are with the Department of Cardiovascular Surgery, Boston Children's Hospital and Harvard Medical School, Boston, MA, 02115 USA first name.lastname@childrens.harvard.edu.

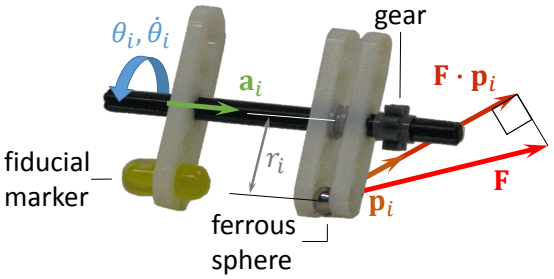

Fig. 1. MRI-powered, single-DOF rotor with fiducial marker and gear for power transmission. remove i subscripts

The contribution of this paper is to develop feedback-control techniques enabling precision control of a rotors. Section III describes an MRI actuator model and control law. Section **??** ends with concluding remarks.

III. FEEDBACK CONTROL

A ferrous particle in the strong static field of an MRI becomes magnetized, and its magnetization magnitude asymptotically approaches the saturation magnetization $\mathbf{M}_s$ per unit volume of the material. The MRI gradient coils produce a magnetic field $\mathbf{B}_g(t)$. This field exerts on the ferrous particle the force

$$\mathbf{F}(t) = v\,(\mathbf{M}_s \cdot \nabla)\,\mathbf{B}_g(t). \tag{1}$$

Here v is the magnetic volume of the material. The magnetic field $\mathbf{B}_g(t)$ is designed to produce three independent gradients:

$$[F_x, F_y, F_z]^\intercal(t) = vM_{sz}\left[\frac{\partial B_{gx}}{\partial z}, \frac{\partial B_{gy}}{\partial z}, \frac{\partial B_{gz}}{\partial z}\right]^\intercal(t) \tag{2}$$

Here it has been reasonably assumed that $M_{sz} \gg M_{sx}, M_{sy}$. These gradients apply three independent forces on any ferromagnetic spheres inside the MRI. The rotor construction constrains the ferromagnetic sphere to rotate about an axis $\mathbf{a}$ with a moment arm of length r, as shown in Fig. 1. The rotor's configuration at time t is fully described by its angular position and velocity $[\theta(t), \dot{\theta}(t)]^\intercal$. The configuration space is $\mathbb{R}^2$, and the dynamic equations are given by

$$\ddot{\theta}(t) = \frac{1}{J}\left(-b\dot{\theta}(t) - \tau_f - \tau_\ell + r\mathbf{F}(t) \cdot \mathbf{p}(t)\right) \tag{3}$$

Here J is the moment of inertia, b the coefficient of viscous friction, τ_f the summation of all non-viscous friction terms seen by the input, and τ_ℓ the load torque. The rotor torque is the magnetic force projected to a vector tangent to the ferrous sphere's positive direction of motion, $r\mathbf{F}\cdot\mathbf{p}(t)$. This model assumes that the rotor is perfectly balanced, and thus there is no gravity-related term. Actuator torque is maximized when $\mathbf{F}(t) = g_M V M_{sz}\,\mathrm{sgn}(\mathbf{p}(t))$, where g_M is the maximum gradient.

When the rotor axis is aligned with a coordinate axis, $\mathbf{p}(t)$ has a particularly simple form. The remainder of the paper will assume $\mathbf{a} = \{0, 1, 0\}$.

$$\ddot{\theta}(t) = \frac{1}{J}\Bigg(- b\dot{\theta}(t) - \tau_f - \tau_\ell + r\Big(F_x(t)\cos(\theta(t)) - F_z(t)\sin(\theta(t))\Big)\Bigg) \quad (4)$$

A. Discrete time model

Both the control and measurements are taken at discrete time intervals, so it is necessary to provide a discrete-time model. This can be obtained by direct integration of (3), or can be approximated by

$$\begin{aligned}\theta(k+1) &= \theta(k) + \dot{\theta}(k)T \\ \dot{\theta}(k+1) &= \dot{\theta}(k) + \frac{T}{J}\Big(-b\dot{\theta}(k) - \tau_f - \tau_\ell + r\mathbf{F}(t)\cdot\mathbf{p}(k)\Big)\end{aligned} \quad (5)$$

with time steps of T seconds.

The position of a nonmoving rotor can be measured by two orthogonal MRI line scans. These line scans measure the rotor's position in 1D. These line scans cannot be measured simultaneously. If the rotor is moving, these scans measure the 1D projection of the rotor's position at two different times:

$$\begin{aligned} y_x(t_1) &= cos(\theta(t_1)) \\ y_z(t_2) &= sin(\theta(t_2)) \end{aligned} \quad (6)$$

Each scan requires $\Delta T = 18$ ms. To minimize movement between scans, the lines scans are taken in succession and $t_2 = t_1 + \Delta T$. The angle measurement is approximated by

$$\theta_{M1}(t_2) \approx \arctan(y_z(t_2), y_x(t_1)) \quad (7)$$

Because these two scans are not taken at the same time, the angular measurement lags the true rotor angle, with maximum errors at $\theta = [\pi/2, 3\pi/2]$.

With two noiseless measurements and an estimate of the current angular velocity $\hat{\dot{\theta}}$, trigonometric inverses can recover the true orientation and velocity. However, discretization errors caused by the MRI's resolution makes trigonometric inverses unreliable. Instead, noting that the lag is periodic with period $2\theta_M$, and amplitude $\frac{\hat{\dot{\theta}}\Delta T}{2}$, the following correction is valid for angular velocities between ± 60 rads/s.

$$\theta_M(t_2) \approx \theta_{M1}(t_2) + \frac{\hat{\dot{\theta}}(t_2)\Delta T}{2}\Big(1 - \cos(2\theta_{M1}(t_2))\Big) \quad (8)$$

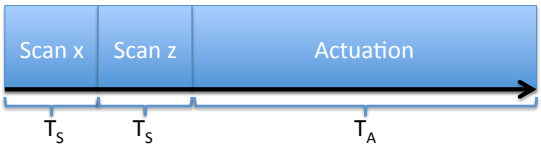

Fig. 2. Timing digram

One approach to state estimation for systems of this type is to linearize the equations about the current estimate and then apply Kalman's equations using the resulting equations. Estimation is split into *predicting* the current state using previous measurements and the process model and *correcting* the estimate using MRI measurements. In between measurements the estimate $\hat{\theta}$ and $\hat{\dot{\theta}}$ as well as the estimate covariance P are predicted by the equations

$$\begin{aligned}\hat{\theta}(k+1|k) &= \hat{\theta}(k|k) + T\hat{\dot{\theta}}(k|k) \\ \hat{\dot{\theta}}(k+1|k) &= \hat{\dot{\theta}}(k|k) + \frac{1}{J}\Big(-b\hat{\dot{\theta}}(k|k) - \tau_f - \tau_\ell \\ &\quad + r\Big(F_x(t)\cos(\hat{\theta}(k|k)) - F_z(t)\sin(\hat{\theta}(k|k))\Big)\Big) \\ P_\theta(k+1|k) &= P_\theta(k|k) + Q_\theta \\ P_{\dot{\theta}}(k+1|k) &= P_{\dot{\theta}}(k|k) + Q_{\dot{\theta}}\end{aligned} \quad (9)$$

The state estimate and covariance are corrected using MRI measurements of the rotor orientation $\theta_M(k+1)$ and a finite difference calculation of the rotor angular velocity $\dot{\theta_M}(k+1)$, along with the measurement noise $R_\theta(k+1)$ and $R_{\dot{\theta}}(k+1)$.

$$\begin{aligned}\hat{\theta}(k+1|k+1) &= \hat{\theta}(k+1|k) + K_\theta(k+1)\Big(\theta_M(k+1) - \hat{\theta}(k+1|k)\Big) \\ \hat{\dot{\theta}}(k+1|k+1) &= \hat{\dot{\theta}}(k+1|k) + K_{\dot{\theta}}(k+1)\Big(\dot{\theta}_M(k+1) - \hat{\dot{\theta}}(k+1|k)\Big) \\ P_\theta(k+1|k+1) &= \Big(1 - K_\theta(k+1)\Big)P_\theta(k+1|k) \\ P_{\dot{\theta}}(k+1|k+1) &= \Big(1 - K_{\dot{\theta}}(k+1)\Big)P_{\dot{\theta}}(k+1|k)\end{aligned} \quad (10)$$

Here $K_\theta(k+1)$ and $K_{\dot{\theta}}(k+1)$ are the optimal Kalman gains

$$\begin{aligned}K_\theta(k+1) &= P_\theta(k+1|k)(P_\theta(k+1|k) + R_\theta(k+1))^{-1} \\ K_{\dot{\theta}}(k+1) &= P_{\dot{\theta}}(k+1|k)(P_{\dot{\theta}}(k+1|k) + R_{\dot{\theta}}(k+1))^{-1}\end{aligned} \quad (11)$$

ACKNOWLEDGEMENTS

This work was supported by the National Science Foundation under IIS-1208509 and by the Wyss Institute for Biologically Inspired Engineering.